

The influence of Holmium-166 loaded microspheres on diffusion weighted imaging: an ex-vivo study

Gerrit H van de Maat¹, Maarten AD Vente², Johannes FW Nijssen², and Chris JG Bakker²

¹Image Sciences Institute, University Medical Center, Utrecht, Utrecht, Netherlands, ²Department of Radiology and Nuclear Medicine, University Medical Center Utrecht, Netherlands

Introduction

Intra-arterial radioembolization (RE), using microspheres that contain a β -emitting radioisotope, is an emerging technique for the treatment of either primary or metastatic liver cancer [1]. One type of microspheres that has been developed for RE and that is currently under investigation in a phase I clinical trial [2] is composed of neutron activated holmium-166 embedded in poly L-lactic acid microspheres (Ho-PLLA-MS). Because of the highly paramagnetic character of holmium, these microspheres are suggested to be an ideal device for MR guided therapy [3]. One part of such an MR guided approach would consist of MRI based treatment follow up to measure tumor response.

A promising MR based approach to assess tumor response is functional imaging by means of Diffusion Weighted Imaging (DWI). It has been shown that DWI enables to distinguish between benign and malignant hepatic lesions, between hepatic abscess and tumor and between necrotic and viable tumor tissue and that DWI can assess tumor response [4]. To measure diffusion, characterized by the apparent diffusion coefficient (ADC), usually a pulsed-gradient spin-echo sequence [5], is used. In this sequence, a pair of (identical) linear gradients is applied symmetric around the π -pulse of a conventional spin-echo sequence. Static spins that are dephased by the first gradient will be rephased by the second gradient but diffusing spins will not entirely be rephased by the second gradient as a consequence of their motion through the applied gradients, resulting in signal loss. The amount of diffusion weighting is controlled by the b-factor: $b = (\gamma G \delta)^2 \cdot (\Delta - \delta/3)$, where γ is the gyromagnetic ratio, G is the gradient strength, δ is the duration of the gradients and Δ the interval between the pulse centers. Using a range of b-values and fitting the mono-exponential function $S = S_0 \cdot \exp[-b \cdot \text{ADC}]$ to the acquired signal intensities, the ADC can be determined. However, assessment of the ADC following this procedure is only valid if there are no other gradients present in the tissue.

Susceptibility variations in tissue induced by the paramagnetic Ho-PLLA-MS will cause field variations leading to non-linear local gradients. Due to these background gradients which add to the diffusion-sensitizing gradients, the MR signal will reduce because of spins diffusing in the local gradients and this can influence the ADC measurements as has been demonstrated using a phantom setup [6]. The purpose of this work was to explore if this influence is large enough to hamper treatment response measurements after radioembolization. This was done using an ex-vivo pig liver into which a non-radioactive therapeutic amount of Ho-PLLA-MS was administered after which ADC changes were measured.

Materials and methods

Preparation: A pig liver was excised, flushed with heparin solution to prevent formation of blood clots and a catheter was introduced into the hepatic artery. A total amount of 500 mg of Ho-PLLA-MS was prepared in 50 ml of MnCl_2 -doped demineralized water. This suspension was then administered to the liver via the catheter and the liver was flushed again with MnCl_2 -doped demineralized water. MR imaging was performed prior to and after administration of Ho-PLLA-MS.

Data acquisition: Diffusion weighted images of the ex-vivo pig liver were acquired using a multi slice spin echo sequence with b-values of 0, 100, 200, 300 and 400 ms/mm^2 with an effective echo time of 54 ms. Other parameters included: repetition time: 1342 ms, field of view: $240 \times 240 \text{ mm}^2$, voxel size: $2.5 \times 2.5 \text{ mm}^2$, slice thickness: 6 mm. To depict the areas in the liver where the Ho-PLLA-MS lodged after administration, T_2^* weighted gradient echo images were acquired (16 echoes) with $\text{TE}_1 = 1.33 \text{ ms}$ and $\Delta\text{TE} = 1.15 \text{ ms}$. Scan parameters included: TR: 400ms, FOV: $256 \times 256 \text{ mm}^2$, voxel size: $2 \times 2 \text{ mm}^2$ and slice thickness: 6mm.

Data processing: From the subsequent diffusion weighted images, ADC maps were constructed by voxel wise fitting the function $S(b) = S(0) \cdot \exp[-b \cdot \text{ADC}]$ to the measured signal intensities using a least squares fitting algorithm. R_2^* maps were constructed from the multi gradient echo dataset by mono-exponentially fitting the intensities of the subsequent gradient echoes to the function $S(\text{TE}) = S(0) \cdot \exp[-R_2^* \cdot \text{TE}]$ using a least squares fitting algorithm. For both fitting procedures an SNR threshold of $S < 3\sigma$ was used where σ was the standard deviation of the signal measured in a region with homogeneous signal intensity and absence of Ho-PLLA-MS. R_2^* maps that were constructed from the data prior to administration were subtracted from the R_2^* maps post-administration after automatic registration using Elastix [7] to yield the increase in R_2^* per voxel since ΔR_2^* relates linearly to the concentration of Ho-PLLA-MS [8]. The same was done for the ADC maps.

Results

No significant differences were observed between DW images of the ex-vivo liver acquired prior to and after administration of HoMS (Figure 1) whereas gradient echo images showed large signal losses at several locations in the liver after administration (Figure 2). R_2^* maps constructed from the multi gradient echo dataset (Figure 3 bottom row) clearly showed increased R_2^* values indicating the presence of Ho-PLLA-MS. However, the patterns of high R_2^* values, visible in these R_2^* maps were not observed in the ADC maps that were constructed from the diffusion weighted images (Figure 3 top row).

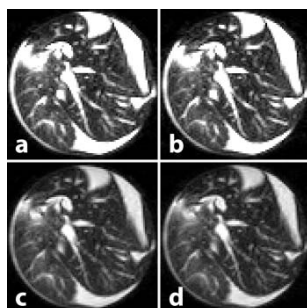


Figure 1. Diffusion weighted images prior to (a, c) and after administration of Ho-PLLA-MS (b, d) for two different b-values (a, b: 0 and c, d: 400 ms/mm^2)

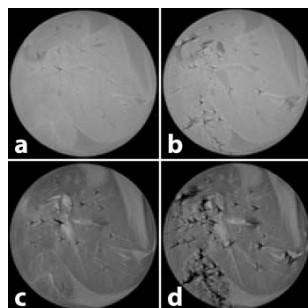


Figure 2. Gradient echo images prior to (a, c) and after administration of Ho-PLLA-MS (b, d) for two different echo times (a, b: 1.33 ms and c, d: 8.23 ms)

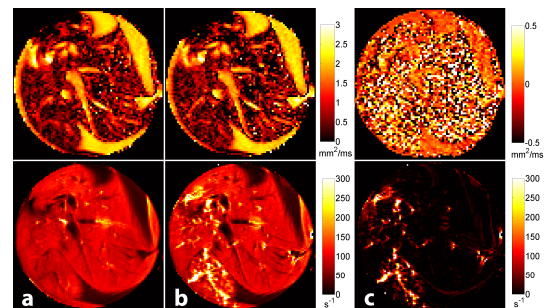


Figure 3. ADC maps (top row) on a scale of 0–3 mm^2/ms and R_2^* maps (bottom row) on a scale of 0–300 s^{-1} prior to (a) and after (b) administration of Ho-PLLA-MS. In (c) the difference between a and b obtained by subtraction is displayed. Here the ADC scale map is $-0.5 - 0.5 \text{ mm}^2/\text{ms}$

Discussion and Conclusion

No significant ADC changes were observed at locations where Ho-PLLA-MS were present in the ex-vivo liver after administration, indicating that ADC measurements are not hampered by the presence of Ho-PLLA-MS, unlike the influence that has previously been demonstrated in a phantom setup [6]. Even at locations where ΔR_2^* values larger than 300 s^{-1} were observed (figure 3 bottom row), corresponding to Ho-PLLA-MS concentrations of more than 3 mg/ml [8], ADC maps showed no evidence of Ho-PLLA-MS influencing the measurements. The reason for this is probably the inherent low SNR of the diffusion weighted images and the intrinsic ADC variations present in the liver tissue which mask possible ADC changes due to Ho-PLLA-MS. Although the amount of administered Ho-PLLA-MS and the MR imaging parameters that were used in this experiment were similar to values that are currently used in clinical practice, so the results approximate the situation that can be expected in-vivo, the obtained results have to be validated in human subjects in the future.

References

- [1] MAD Vente et al. Eur Radiol 2009;19:951-959 [2] MLJ Smits et al. J Exp Clin Cancer Res 2010;29:70 [3] JFW Nijssen et al. Radiology 2004;231:491-499 [4] B Taouli and D Koh. Radiology 2010;254:47 [5] EO Stejskal and JE Tanner. J Chem Phys 1965;42:228-292 [6] GH van de Maat et al. Proc Int Soc Magn Res Med 2010 [7] S Klein et al. IEEE Trans Med Imag 2010;29:196-205 [8] PR Seevinck et al. MRM 2008;60:1466-1476